



Study of Conversion of Waste Jarosite Precipitates to Hematite

Hong Nguyen VU¹⁾, Petr DVOŘÁK²⁾, Tomáš SÍTA³⁾

¹⁾ Ph.D., Ing.; Institute of Chemical Technology (ICT), Technická 5, 16628 Prague 6, Czech Republic; corresponding author, tel: +420-2-2044 5025, fax: +420-2-2044 4400, email: vun@vscht.cz

²⁾ Ph.D., Ing.; Department of Metals and Corrosion Engineering, Prague Institute of Chemical Technology, Prague, Technická 5, 16628 Prague 6, Czech Republic; email: dvorakp@vscht.cz

³⁾ Department of Metals and Corrosion Engineering, Prague Institute of Chemical Technology, Prague, Czech Republic

Summary

Sodium and ammonium jarosite precipitates from the sulfuric acid leaching of deep-sea nodules were converted into well crystallized hematite by alkali decomposition of jarosite using sodium hydroxide or ammonia solutions at different temperature and subsequent sintering at 400 and 750°C. The obtained sodium and ammonium jarosite precipitates were intergrown aggregates composed of half-prism and tabular-like crystals with sharp corners and edges. It was found that base-strength of alkali solutions effected the kinetics of conversion reactions and morphology of solid phase. The residual solids retained the shape and the particle size of the original jarosite precipitates. The main feature of the residual from sodium jarosite is a severe surface pitting and an erosion of edges and corners. The decomposition of ammonium jarosite precipitates at different temperatures took place very fast and completed within 15 minutes at 25°C. Increasing temperature increased the decomposition rate. At 60°C jarosite decomposition was completed in less than 2 minutes. But the experimental results indicated that the sulfate anions slowly diffused from the jarosite structure after the completion of the decomposition reaction. The main impurities in jarosite precipitates such as Mn, Cu and Ni reported into the final product but hematite obtained from decomposition of ammonium jarosite contained significantly less Cu due to formation of copper ammonia complex. The XRD analysis results indicated that the decomposition products at temperatures lower than 90°C are amorphous. At 90°C the decomposition products consisted of poorly crystallized hematite. After sintering the decomposition products from both sodium and ammonium jarosites at 400°C and 750°C, well-crystallized hematite was obtained.

Keywords: aqueous conversion, deep-sea nodules, jarosite, iron oxides

Introduction

Jarosite precipitation using an alkali, such as ammonia, sodium or potassium as $\text{MeFe}_3(\text{SO}_4)_2(\text{OH})_6$ ($\text{Me}=\text{K}^+$, NH_4^+ , H_3O^+ etc.) is the most common process to remove iron from leach liquors in the zinc industry. The main advantages of precipitating jarosite compounds are the high precipitation efficiency and ease of filtration. It also allows the process to be carried out at lower temperatures and in strongly acidic media, which avoids the expensive neutralization step. This jarosite precipitate however, often includes small amounts of lead, arsenic, cadmium and mercury (Ismael and Carvalho, 2003; Moors, 2000; Dutrizac and Jambor, 2000) and co-precipitation of the divalent base metals such as Cu^{2+} , Zn^{2+} , Co^{2+} , has also been reported (Dutrizac, 1982). For the above reasons the jarosite precipitate waste is one of the biggest environmental problems in the zinc production industry.

Several hydrometallurgical jarosite treatment routes have been investigated to prepare hematite and magnetite. Kunda and Veltman studied three treatments of ammonium jarosite: thermal decomposition with recovery of hematite, decomposition in an aqueous slurry to hematite and/or magnetite; and defined the decomposition conditions of all three methods (Kunda and Veltman, 1979). Dutrizac investigated the hydrothermal conversion of sodium jarosite to hematite and established the time-temperature relationships for the conversion reaction (Dutrizac, 1989). Bohacek et al. prepared black pigments (Fe_3O_4) by the neutralization of the hydronium jarosite suspension in FeSO_4 aqueous solutions with NH_3 and the subsequent thermal treatment of this mixture at controlled pH and temperature (Bohacek et al.,

1993). The production of magnetite from synthetic sodium jarosite using MgO as a neutralizing agent and pure acid-washed cellulose as a reducing agent was described by Hage et al. (1999).

The objective of the present study is to produce pigment-quality hematite from unique sodium and ammonium jarosite, which were precipitated from manganese sulfate leach liquors obtained from acidic leaching deep sea nodules. The conversion was carried out by alkali decomposition of sodium and ammonium jarosite in sodium hydroxide and ammonia solutions, respectively. The conversion time, morphological, mineralogical and chemical changes of solid phase during conversion were investigated.

Experimental

Materials

Jarosite compounds used in this study were precipitated from leach solutions which were prepared by leaching deep-sea nodules in $\text{FeSO}_4\text{-H}_2\text{O-H}_2\text{SO}_4$ media under experimental conditions as determined in our previous study (Jandova et al., 2001, Vu et al., 2005). All chemicals used were of analytical grade and supplied by Pentachemicals Ltd.

Experimental procedure

The conversion experiments were carried out in a 1-L glass reactor fitted with a condenser and a thermometer, heated with a mantle controlled by a regulator and agitated with a mechanical stirrer. At first the suspension of 33.7 g jarosite in 175 mL H_2O was heated up and then 76 mL of 25% w. NaOH or 76 mL of 25% w. aqueous ammonia was

Tab. 1 Content of selected metals in jarosite precipitates
 Tab. 1 Zawartość wybranych metali w wytrąconym jarosycie

| Jarosite | % Fe | % Mn | % Ni | % Co | % Cu |
|-----------------|-------|------|-------|-------|------|
| Na | 33.96 | 0.21 | <0.01 | <0.01 | 0.23 |
| NH ₄ | 33.94 | 0.16 | <0.01 | <0.01 | 0.15 |

Tab. 2 A change of pH values of reaction mixtures at different temperature/ammonium jarosite
 Tab. 2 Zmiana wartości pH w reakcji mieszanin w różnych temperaturach/jarosyt amonu

| Temp. | Time [min] | | | | | | | | |
|-------|------------|-------|-------|-------|-------|-------|-------|-------|------|
| | 0 | 1 | 2 | 3 | 4 | 5 | 10 | 15 | 20 |
| 25°C | 12.11 | 11.28 | 10.90 | 10.68 | 10.54 | 10.42 | 10.16 | 10.03 | 9.96 |
| 40°C | 11.52 | 9.79 | 9.53 | 9.39 | 9.32 | 9.27 | 9.18 | 9.17 | 9.16 |
| 60°C | 11.04 | 8.75 | 8.64 | 8.61 | 8.60 | 8.61 | 8.62 | 8.63 | 8.62 |

Tab. 3 Content of main elements in iron oxides obtained at different reaction temperatures [%]
 Tab. 3 Zawartość głównych elementów tlenku żelaza w różnych temperaturach reakcji [%]

| Jarosite | Temperature [°C] | Fe | Cu | Mn | Ni | Co | S |
|----------|------------------|-------|------|------|------|------|------|
| Sodium | 25 | 63.71 | 0.38 | 0.38 | 0.02 | 0.02 | - |
| | 40 | 63.66 | 0.4 | 0.40 | 0.02 | 0.02 | - |
| | 60 | 63.44 | 0.39 | 0.39 | 0.02 | 0.01 | - |
| | 90 | 63.53 | 0.43 | 0.43 | 0.02 | 0.02 | - |
| Ammonium | 25 | 63.09 | 0.07 | 0.27 | 0.01 | 0.01 | 0.94 |
| | 40 | 65.72 | 0.08 | 0.29 | 0.01 | 0.02 | - |
| | 60 | 65.71 | 0.11 | 0.28 | 0.02 | 0.02 | - |
| | 90 | 65.07 | 0.12 | 0.32 | 0.02 | 0.02 | - |

Tab. 4 Content of main elements in decomposition products versus reaction time: 40°C [%]
 Tab. 4 Zawartość głównych elementów w produktach rozkładu wobec czasu reakcji: 40°C [%]

| Jarosite | Time [min] | Fe | Cu | Mn | Ni | Co | S |
|----------|------------|-------|------|------|------|------|------|
| Sodium | 2 | 55.24 | 0.35 | 0.35 | 0.02 | 0.01 | 1.5 |
| | 6 | 50.44 | 0.34 | 0.35 | 0.02 | 0.01 | 1.64 |
| | 13 | 54.19 | 0.37 | 0.36 | 0.01 | 0.02 | 1.35 |
| | 15 | 54.42 | 0.37 | 0.36 | 0.02 | 0.01 | 1.6 |
| | 30 | 54.56 | 0.36 | 0.36 | 0.03 | 0.01 | 1.48 |
| | 60 | 55.79 | 0.36 | 0.37 | 0.02 | 0.01 | 1.39 |
| | 90 | 54.99 | 0.37 | 0.37 | 0.02 | 0.01 | 1.57 |
| | 420 | 63.13 | 0.42 | 0.42 | 0.02 | 0.02 | 0.07 |
| Ammonium | 2 | 50.42 | 0.11 | 0.21 | 0.01 | 0.01 | 5.91 |
| | 5 | 55.70 | 0.11 | 0.22 | 0.01 | 0.01 | 4.18 |
| | 7 | 58.95 | 0.11 | 0.22 | 0.01 | 0.01 | 3.29 |
| | 10 | 58.09 | 0.11 | 0.23 | 0.01 | 0.01 | 2.92 |
| | 15 | 58.39 | 0.12 | 0.24 | 0.01 | 0.01 | 2.79 |
| | 30 | 61.89 | 0.11 | 0.23 | 0.01 | 0.01 | 2.18 |
| | 60 | 61.60 | 0.12 | 0.23 | 0.01 | 0.01 | 1.95 |
| | 90 | 61.07 | 0.11 | 0.23 | 0.01 | 0.01 | 1.92 |
| | 420 | 64.66 | 0.07 | 0.29 | 0.01 | 0.02 | 0.08 |

added. Samples were collected at selected time intervals and filtered off. Solid phase was analysed for mineralogical composition and chemical attack, and the liquor analysed for sulphate concentration. After the reaction mixture was cooled to the laboratory temperature, the products were separated by filtration, washed and dried at 90°C in an air oven. Same prepared iron oxides were subjected to thermal treatment in a muffle furnace at 400 and 750°C for 3h.

Analysis

Solution and solid samples from alkali decomposition and magnetite formation were analysed using a GBC atomic absorption spectrophotometer (model GBC 932 plus) to determine metals composition. For elemental analysis of solid samples, approximately 0.25g of jarosite or magnetite were dissolved in 20 ml of 10% HCl. The solutions were then diluted to 100 mL with 5% H₂NO₃. Mineralogical analysis was undertaken with X-ray diffraction (PANalytical's X'Pert PRO) using Cu radiation and surface analysis was undertaken with a Scanning Electron Microscope (Hitachi S4700). The particle size distribution of jarosite and magnetite samples were measured by a laser sizer (Frisch, Analysette 22) using Fraunhofer approximation software. Sulfur content in jarosite and magnetite samples was determined using a total sulfur/chlorine analyser (Mitsubishi TOX-100) where samples were burned in an argon/oxygen atmosphere and the resulting sulfur dioxide was auto-titrat-

ed coulometrically with triiodine. Sulfate concentration in solution was determined gravimetrically using 10% BaCl₂ solution.

Results and discussion

Characterization of jarosite precipitates

XRD analysis showed that only the jarosite-group compounds were synthesized (Fig. 1). Chemical analysis of the jarosite precipitates found that the main impurities were copper and manganese, as shown in Table 1.

The strong co-precipitation of copper with iron is in agreement with findings by Dutrizac (1982). A high content of divalent manganese in jarosite precipitates, similar to that of copper, was a result of a higher manganese concentration in leach liquors. Incorporation of nickel, cobalt and titanium into jarosite is negligible. Sodium and ammonium jarosite precipitates are intergrown aggregates composed of half-prism and tabular-like crystals with sharp corners and edges, as shown in Figures 2 a-c.

Alkali decomposition of jarosite precipitates to iron oxides

The alkali decomposition of jarosite takes place according to the following reaction (Salinas et al., 2001):

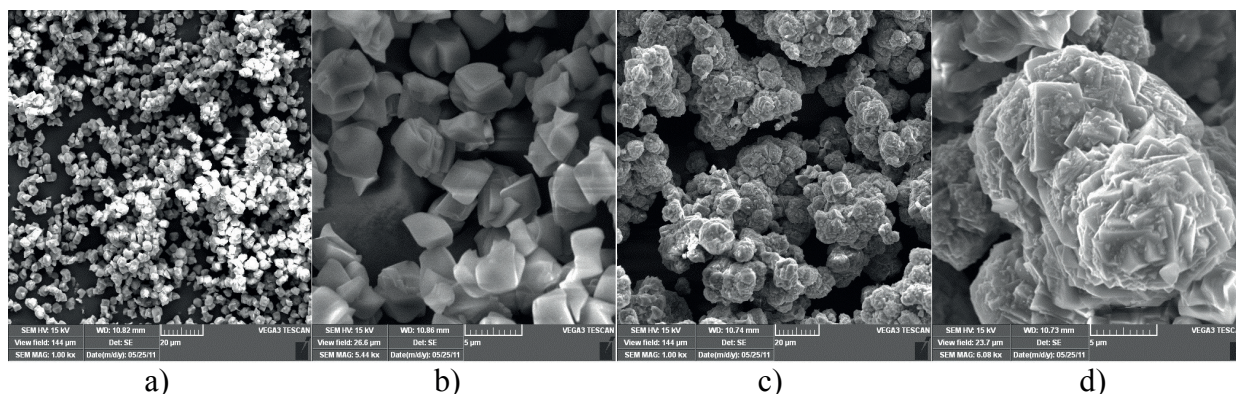
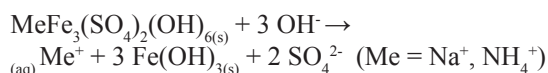


Fig. 2 SEM image of sodium (a,b) and ammonium (c,d) jarosite precipitates at different magnification

Rys. 2 Obraz SEM sodu (a, b) i amonu (c, d) wytrąconego jarosytu w różnym powiększeniu

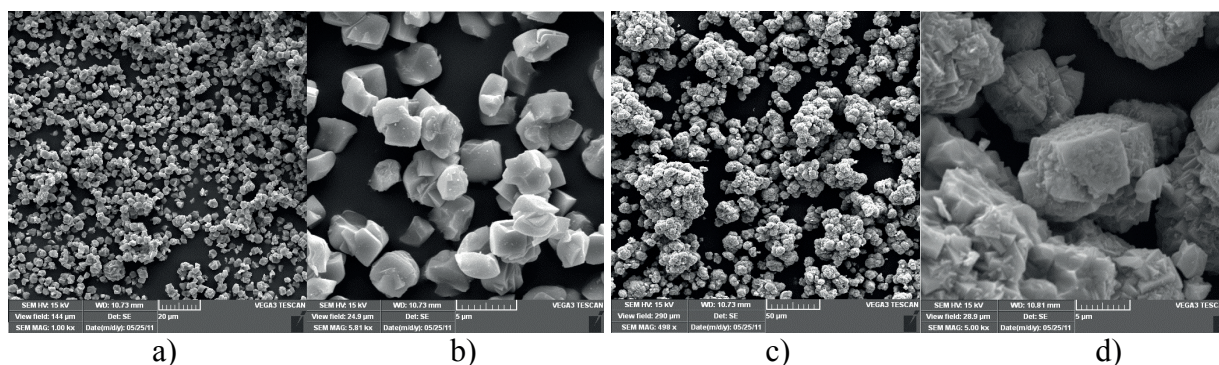


Fig. 3 SEM images of iron oxides prepared from sodium jarosite (a-b) and ammonium jarosite (c-d): 90°C, 7h

Rys. 3 Obraz SEM tlenku żelaza złożonego z jarosytu sodu (a-b) i jarosytu amonu (c-d): 90°C, 7h

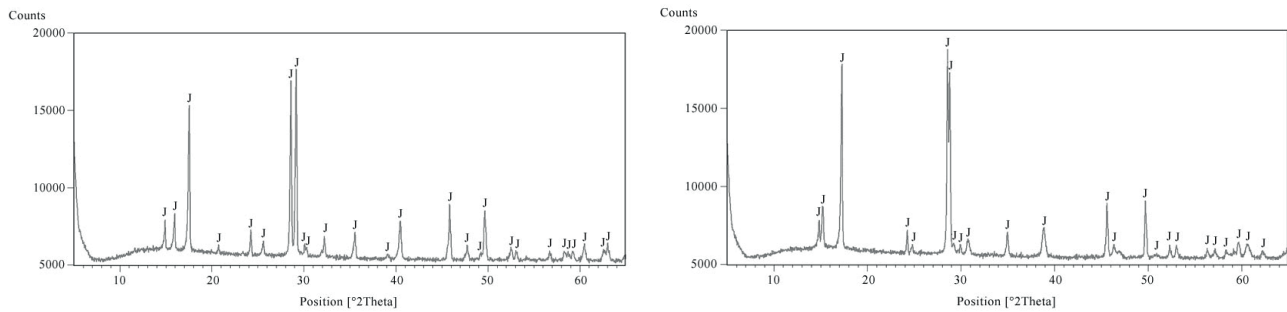


Fig. 1 XRD patterns of jarosite precipitate: a) – $\text{NaFe}_3(\text{SO}_4)_2(\text{OH})_6$; b) – $\text{NH}_4\text{Fe}_3(\text{SO}_4)_2(\text{OH})_6$
 Rys. 1 Schemat XRD wytrąconego jarosytu a) – $\text{NaFe}_3(\text{SO}_4)_2(\text{OH})_6$; b) – $\text{NH}_4\text{Fe}_3(\text{SO}_4)_2(\text{OH})_6$

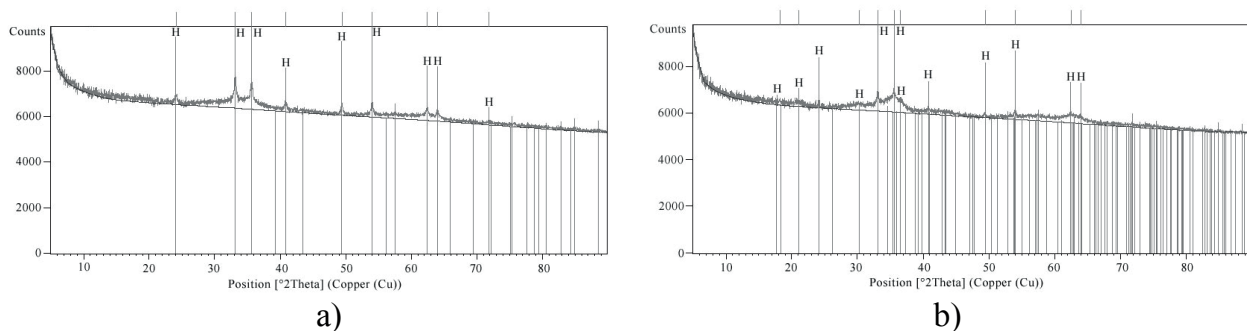


Fig. 4 XRD patterns of iron oxides prepared from ammonium jarosite (a) and sodium jarosite (b): 90°C, 7h
 Rys. 4 Schemat XRD tlenku żelaza złożonego z jarosytu amonu (a) i jarosytu sodu (b): 90°C, 7h

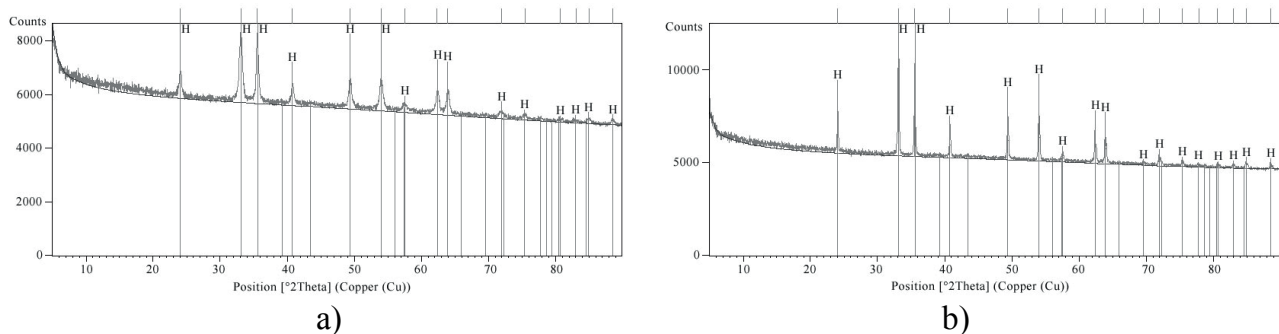


Fig. 5 XRD patterns of iron oxides from ammonium jarosite, sintered at (a) 400 and (b) 750°C
 Rys. 5 Schemat XRD tlenku żelaza z jarosytu amonu, podgrzanego do (a) 400 i (b) 750°C

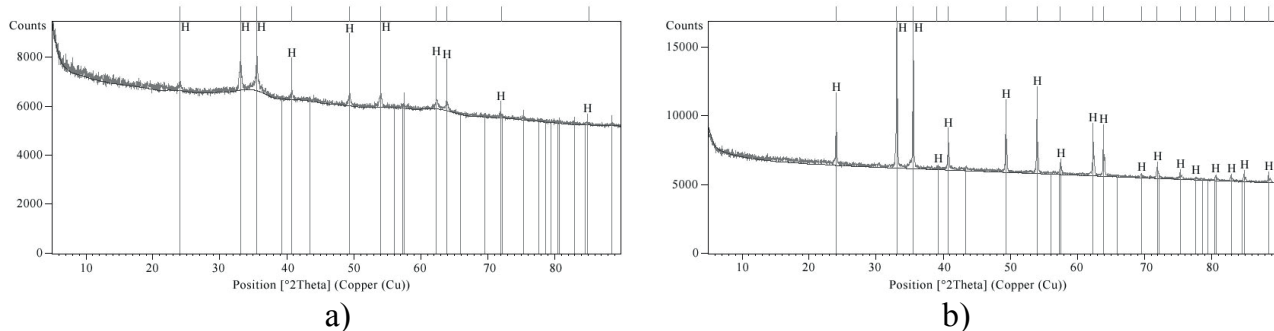


Fig. 6 XRD patterns of iron oxides from sodium jarosite, sintered at (a) 400 and (b) 750°C
 Rys. 6 Schemat XRD tlenku żelaza z jarosytu sodu, podgrzanego do (a) 400 i (b) 750°C

The amount of OH⁻ anions consumed by the decomposition reaction resulted in decreasing pH values of the reaction mixture. As shown in Tab. 2, the decomposition of ammonium jarosite precipitates at different temperatures took place very fast and completed within 15 minutes at 25°C. Increasing temperature increased the decomposition rate. At 60°C jarosite decomposition was completed in less than 2 minutes. The decomposition of sodium jarosite occurred immediately even at laboratory temperature. On the other hand, the sulfur content in both types of jarosites decreased slowly with reaction time and achieved the steady state after 7h (Tab. 4). These results indicated that the sulfate anions slowly diffused from the jarosite structure after the completion of the decomposition reaction. The summary of the elemental content of decomposition products at different temperatures is shown in Tab. 3. All impurities from jarosite precipitates reported to the decomposition products except lower content Cu of those from ammonium jarosite as a result of copper ammonia complexation.

SEM images of reacted particles of sodium and ammonium jarosite after 420 min decomposition are shown in Figure 3 a-b and c-d, respectively. Generally, the residual solids retained the shape and the particle size of the original jarosite precipitates. The main feature of the residual from sodium jarosite is a severe surface pitting and an erosion of edges and corners. This is evidently a result of the strong base nature of sodium hydroxide. In contrast the reacted particles from ammonium jarosite look identical as their original jarosite. At higher magnification, a mild surface

pitting, which is probably caused by the weak base nature of ammonia solution, was revealed.

The XRD analysis results indicated that the decomposition products at temperatures lower than 90°C are amorphous. At 90°C the decomposition products consisted of poorly crystallized hematite (Fig. 4 a-b). Well crystallized hematite was obtained after sintering the decomposition products from both sodium and ammonium jarosites at 400°C and 750°C (Fig. 5-6).

Conclusions

1. The alkali decomposition of jarosite was very fast and completed within 15 min after the addition of aqueous alkali solutions. The solid residuals are mainly amorphous in nature with similar shape and particle size as their original jarosite precipitates.
2. Higher temperature led to a higher decomposition rate and an increase in crystallinity of ferric oxide. Sulfate anions diffused slowly from the jarosite structure after the completion of the alkali decomposition.
3. Well crystallized hematite was obtained by sintering the decomposition products – iron oxides at 400 and 750°C. Higher sintering temperature resulted in higher crystallinity of hematite.

Acknowledgement

The work was supported by the Interoceanmetal, Joint Organization, Szczecin, Poland and by the Research intention MSM No. 223100002.

Literatura - References

1. Bohacek, J., Subrt, J., Hanslik, T., Tlaskal, J. Preparing particulate magnetites with pigment properties from suspensions of basic iron(III) sulfates with the structure of jarosite. *J. Materials Science*. 1993, 28(10), 2827-2832. ISSN 0022-2461.
2. Dutrizac, J. E., Jambor, J.L. Jarosites and their application in hydrometallurgy. *Reviews in Mineralogy and Geochemistry*. 2000, 40(Sulfate Minerals), 405-452. ISSN 1529-6466.
3. Dutrizac, J.E. Jarosite-type compounds and their application in the metallurgical industry. In: *Hydrometallurgy: Research, Development and Plant Practice, Proceedings of International Symposium, 3rd*. Warrendale, PA, USA: The Metallurgical Society of AIME, 1982. pp. 531-551. ISBN 978-0895204561.
4. Dutrizac, J.E. The hydrothermal conversion of jarosite-type compounds to hematite. In: *Productivity and Technology in the Metallurgical Industries*. Warrendale, PA: TMS-AIME, 1989. pp. 587-612.
5. Hage, J.L.T, Schuiling, R.D., Vriend, S.P. Production of magnetite from sodium jarosite under reducing hydrothermal conditions. The reduction of Fe³⁺ to Fe²⁺ with cellulose. *Canadian Metallurgical Quarterly*. 1999, 38(4), 267-276. ISSN 0008-4433.
6. Ismael, M.R.C., Carvalho, J.M.R. Iron recovery from sulfate leach liquors in zinc hydrometallurgy. *Minerals Engineering*. 2003, 16(1), 31-39. ISSN 0892-6875.
7. Jandova, J., Vu, H., Lisa, K., Grygar, T., Bohacek, J. Hydrometallurgical processing of manganese deep-sea nodules: Dissolution and iron recovery. In: *The Proceedings of The Fourth (2001) ISOPE OCEAN MINING SYMPOSIUM*. Cupertino, CA, USA: ISOPE, 2001. pp. 167-171. ISBN 978-1-880653-56-2.
8. Kunda, W., Veltman, H. Decomposition of jarosite. *Metallurgical Transactions B: Process Metallurgy*. 1979, 10B(3), 439-446. ISSN 0360-2141.
9. Moors, E.H.M. *Metal Making in Motion - Technology Choices for Sustainable Metals Production*. Delft, the Netherlands: Delft University Press, 2000. Dissertation. Delft University of Technology, Faculty of Technology, Policy and Management. ISBN 90-407-2075-4.
10. Salinas, E., Roca, A., Cruells, M., Patino, F., Cordoba, D.A. Characterization and alkaline decomposition-cyanidation kinetics of industrial ammonium jarosite in NaOH media. *Hydrometallurgy*. 2001, 60(3), 237-246. ISSN 0304-386X.
11. Vu, H., Jandová, J., Lisá, K., Vranka, F. Leaching of manganese deep ocean nodules in FeSO₄-H₂SO₄-H₂O solutions. *Hydrometallurgy*. 2005, 77(1-2), 147-153. ISSN 0304-386X.

Badania nad konwersją wytrąceń jarosytu w hematyt

Sodowy i amonowy jarosyt wytrąca się podczas ługowania kwasem solnym guzków głębinowych i zostaje przetworzony w wyraźnie skryształizowany hematyt za pomocą dekompozycji alkalicznej jarosytu, która zachodzi przy użyciu wodorotlenku sodu lub roztworów amonowych w różnych temperaturach oraz następujących potem procesów spiekania w 400 i 750°C. Uzyskane wytrącenia sodowego i amonowego jarosytu utworzyły następnie skupienia złożone z pół-pryzmatycznych i tabularycznych kryształów o ostrych końcach i krawędziach. Stwierdzono, że siła roztworów alkalicznych wpływa na kinetykę reakcji konwersji oraz morfologię fazy stałej. Pozostałe części stałe utrzymały kształt i wielkość ziaren oryginalnego wytrącenia jarosytu. Główną cechą reszt z sodowego jarosytu są wżery powierzchniowe oraz erozja krawędzi i końców. Dekompozycja wytrąceń jarosytu amonowego zachodzi bardzo szybko w innej temperaturze. Zajmuje to nie więcej jak 15 minut w temperaturze 25°C. Wzrost temperatury powoduje wzrost stopnia dekompozycji. W temperaturze 60°C dekompozycja jarosytu została ukończona w czasie mniejszym niż 2 minuty. Jednakże, wyniki eksperymentu wskazały, że aniony siarczanowe ulegają powolnej dyfuzji ze struktury jarosytu po ukończeniu reakcji rozkładu. Głównymi zanieczyszczeniami w wytrąceniach jarosytu są takie pierwiastki jak Mn, Cu oraz Ni, których obecność stwierdzono w finalnym produkcie. Jednak hematyt otrzymany w wyniku dekompozycji jarosytu amonowego zawierał znacznie mniej Cu ze względu na utworzenie kompleksu amonowego miedzi. Wyniki analizy XRD wykazały, że produkty rozkładu w temperaturze niższej niż 90°C są amorficzne. W temperaturze 90°C produkty rozkładu zawierały słabo skryształizowany hematyt. Po spiekaniu produktów rozkładu z zarówno sodowego, jak i amonowego jarosytu w temperaturach 400°C oraz 750°C otrzymano dobrze skryształizowany hematyt.

Słowa kluczowe: konwersja wodna, guzki głębinowe, jarosyt, tlenki żelaza